NAVY DEPARTMENT
THE DAVID W. TAYLOR MODEL BASIN
WASHINGTON 7, D.C.

THE STATIC STABILITY DERIVATIVES OF A SERIES OF RELATED BODIES OF REVOLUTION

by

J.L. Johnson

March 1951

96

Report C-383

[redacted]

[redacted] 62

ERRATA SHEET

for

David Taylor Model Basin Report C-383

The following changes are to be made in Report C-383:

Page 6, Figure 3 - Invert left-hand scale (Lift in lb), placing the negative quantities on top.

Page 12, Line 21 - Change $1/2\ \rho\ U^2\ \forall^3$ to $1/2\ \rho\ U^2\ l^3$.

Page 14, Line 21 - Change the phrase:

> "Differentiating the numerator and denominator with respect to w and allowing w to approach zero, we have the limiting position"

to read as follows:

> "Inasmuch as the curves of M' and Z' against α are linear near the origin and as by symmetry they pass, or can be made to pass, through the origin, we may differentiate the preceding numerator and denominator with respect to w' and allow w' to approach zero to give the limiting position"

[redacted]

INITIAL DISTRIBUTION

Serials	
1 - 13	Chief, BuShips, Project Records (Code 324), for distribution: 1 - 5 Project Records 6 Deputy and Assistant Chief (Code 101) 7 Technical Assistant to the Chief (Code 106) 8 Research (Code 300) 9 Ship Design (Code 410) 10 - 11 Preliminary Design (Code 420) 12 Submarines (Code 515) 13 Electronics Design, Oceanography (Code 847), for Mr. Allyn Vine
14 - 17	Chief, BuShips, Steering Gear, Hoisting Machines and Utilities (Code 622), for distribution: 14 Mr. Stine 15 Askania Regulator Company 16 Sperry Gyroscope Company 17 Eclipse-Pioneer Division of Bendix Aviation Corporation
18 - 19	Director, Langley Aeronautical Laboratory, Langley Air Force Base, Langley Field, Va.
20	Commander, Submarine Force, U.S. Atlantic Fleet
21	Commander, Submarine Force, U.S. Pacific Fleet
22	Commander, Portsmouth Naval Shipyard
23	Commander, Mare Island Naval Shipyard
24	Supervisor of Shipbuilding, USN, and Naval Inspector of Ordnance, Electric Boat Company, Groton, Conn.
25 - 26	Commander, Naval Ordnance Laboratory, White Oak, Silver Spring, Md.
27	Development Contract Officer, Kellex Corporation, for Director, Silver Spring Laboratory, The Kellex Corporation
28	Commander, Naval Ordnance Test Station, Inyokern, Calif.
29	Commanding Officer, U.S. Naval Torpedo Station, Newport, R.I.
30	Inspector of Naval Material, 1206 So. Santee St., Los Angeles, Calif., for Director, Hydrodynamics Laboratories, California Institute of Technology, Pasadena, Calif.
31 - 32	Chief of Naval Research, 31 Naval Sciences Division 32 Mathematical Sciences Division
33	Assistant Chief of Naval Operations (Undersea Warfare Division)
34	Chief, BuAer, Aero and Hydrodynamics (DE-3)
35	Commander, Naval Ordnance Test Station, Underwater Ordnance Division, Pasadena, Calif.
36	Director, Experimental Towing Tank, Stevens Institute of Technology, Hoboken, N.J.
37 - 43	Members of the Panel on the Hydrodynamics of Submerged Bodies, Committee on Undersea Warfare, National Research Council 37 INSMAT, 1050 Broad St., Newark, N.J., for Dr. K.S.M. Davidson, Chairman, Stevens Institute of Technology, 711 Hudson St., Hoboken, N.J.

38 Supervisor of Shipbuilding, USN, and Naval Inspector of Ordnance, Electric Boat Company, Groton, Conn., for Rear Adm. A.I. McKee, USN (Ret.)

39 Vice Adm. E.L. Cochrane, USN (Ret.), U.S. Maritime Administration

40 INSMAT, 401 Water St., Baltimore 2, Md., for Dr. G.F. Wislicenus, Dept. of Mechanical Engineering, Johns Hopkins University, Baltimore, Md.

41 Supervisor of Shipbuilding, USN, and Naval Inspector of Ordnance, 11 Broadway, New York 4, N.Y., for Rear Adm. P.F. Lee, USN (Ret.), Gibbs & Cox, Inc., New York 4, N.Y.

42 Mr. F.L. Thompson, NACA, Langley Air Force Base, Langley Field, Va.

43 Captain W.S. Diehl, USN, Bureau of Aeronautics

44 Commanding Officer, U.S. Naval Training Schools, Massachusetts Institute of Technology, Cambridge, Mass.

THE STATIC STABILITY DERIVATIVES OF A SERIES OF RELATED BODIES OF REVOLUTION

by

J.L. Johnson

March 1951

Report C-383

TABLE OF CONTENTS

NOTATION

The terminology used in this report is in general agreement with the provisions of Reference 3. The longitudinal, lateral and vertical axes x, y, and z, respectively, through the center of buoyancy are assumed to rotate with the ship. Positive directions are x forward, y to starboard and z downward, perpendicular to x and y. The corresponding forces and velocities are denoted by X, Y and Z and u, v and w, respectively. Moment M and angle of attack α about the y axis are assumed positive in the sense of the right-hand rule.

Following is a summary of symbols used. The prime used in the text indicates the respective nondimensional form. For convenience, certain of these symbols are defined symbolically in the succeeding section.

a	Distance of lift vector from center of buoyancy, measured along the x axis
C_p	Prismatic coefficient
C_s	Wetted-surface coefficient
C_t	Total-resistance coefficient
D	Drag force (total resistance)
d	Diameter of body
h	Depth from surface to centerline of model
L	Lift force
L_w	Static-lift derivative, experimental value
L_{we}	Static-lift derivative, empirical
l	Length of body
M	Moment about y axis
M_i	Ideal-fluid moment about y axis
M_w	Static-moment derivative, experimental
M_{we}	Static-moment derivative, empirical
M_{wi}	Static-moment derivative, ideal-fluid value
m	Mass of displaced fluid
r_0	Nose-radius coefficient
r_1	Tail-radius coefficient
S	Wetted surface of body
U	Velocity of origin relative to fluid
$\forall$	Volume of body
w	Velocity in Z direction
$\bar{x}$	Position of bow relative to center of buoyancy

UNCLASSIFIED

Z	Normal force, positive downwards
Z_w	Static normal-force derivative
α	Angle of attack, in radians
δ	Distance of lift vector from center of buoyancy, measured along the x axis
ξ_m	Position of maximum section
ρ	Mass density of fluid

DEFINITIONS

$$a' = \frac{a}{l}$$

$$C_p = \frac{\forall}{\frac{\pi d^2}{4} l}$$

$$C_s = \frac{S}{\pi l d}$$

$$C_t = \frac{D}{\frac{1}{2}\rho U^2 S}$$

$$L' = \frac{L}{\frac{1}{2}\rho U^2 l^2}$$

$$L'_w = \lim_{w' \to 0} \frac{\partial L'}{\partial w'} = \lim_{\alpha \to 0} \frac{\partial L'}{\partial \alpha}$$

$$M' = \frac{M}{\frac{1}{2}\rho U^2 l^3}$$

$$M'_w = \lim_{w' \to 0} \frac{\partial M'}{\partial w'} = \lim_{w' \to 0} \frac{\partial M'}{\partial \alpha}$$

$$m' = \frac{2\forall}{l^3}$$

$$r_0 = \frac{(\text{nose radius})\, l}{d^2}$$

$$r_1 = \frac{(\text{tail radius})\, l}{d^2}$$

$$w' = \frac{w}{U}$$

$$\overline{x} = \frac{x_{bow}}{l}$$

$$Z = -(L \cos \alpha + D \sin \alpha)$$

$$Z' = \frac{Z}{\frac{1}{2}\rho U^2 l^2}$$

$$Z'_w = \lim_{w' \to 0} \frac{\partial Z'}{\partial w'} = \lim_{\alpha \to 0} \frac{\partial Z'}{\partial \alpha}$$

$$= -(L'_w + D')$$

$$\delta' = a' - \overline{x}$$

$$\xi_m = \frac{x_{bow} - x_{\text{max. section}}}{l}$$

ABSTRACT

This report describes static stability tests performed on a series of axially symmetric bodies of systematically varied form. Lift and moment derivatives are plotted as a function of form and approximate empirical relationships between derivatives and form are cited.

INTRODUCTION

The work described herein was authorized by the Bureau of Ships[1] as part of a program to develop improved forms for undersea propulsion. The results obtained, however, may be considered of general application in the linearized stability analysis of bodies in incompressible flow.

The increased importance of high submerged speed has posed new directional-stability problems due to the decreased time required for the ship to stray from a desired course. Snorkelling and the present limits of safe submergence both impose severe restrictions on allowable depth variation.

Static stability, determined by towing at fixed angles of attack, is measured by the derivative, with respect to angle of attack, of the pitching moment about the center of gravity. In these tests it has been assumed that the centers of gravity and volume coincide. A positive value of this quantity indicates instability, as the hydrodynamic moment then acts in such a direction as to increase the angle. This implies that the center of pressure is ahead of the center of volume. The greater the positive value of this derivative, the greater the instability. All known elongated bodies of revolution are statically unstable, the degree of such instability depending on the shape. Increased static stability is obtained by moving the center of pressure aft. Normally this is done by adding stabilizing surfaces at the stern.

Dynamic stability, measured by the stability index, σ, which determines the rate of decay of a small disturbance, is also a function of hull form and of size and location of stabilizing surfaces. It is conceivable that a hull of minimum drag may not necessarily be the optimum form when the drag of appendages required for stability is included. A separate report will describe a method for determining the appendage area required to obtain a desired stability index. As a preliminary phase and a source of information required in the computation of dynamic stability, the present report is concerned entirely with static-stability derivatives of the bare hull alone.

---

[1]References are listed on page 18.

These derivatives were obtained for twenty-three bodies involving systematic variation of the following form parameters:

1. Length-diameter ratio, l/d
2. Position of maximum ordinate, ξ_m
3. Prismatic coefficient, C_p
4. Nose radius, r_0
5. Tail radius, r_1

For reference, the resistance values for each model as obtained in these tests are given in this report; however it is recommended that for all practical applications the more precise values of Reference 2 be used.

DESCRIPTION OF MODELS

The models, designated as TMB Series 58, were of orthodox laminated wood construction, finished with clear enamel and polished to a high gloss. One was of sugar pine and one Alaska cedar. The rest were mahogany. All models were 9 feet in length, with diameters ranging from 10 to 27 inches. A typical model is shown in Figure 1. The sand strip shown was used only for special tests performed on Models 4164, 4166, and 4177. Geometrical data for

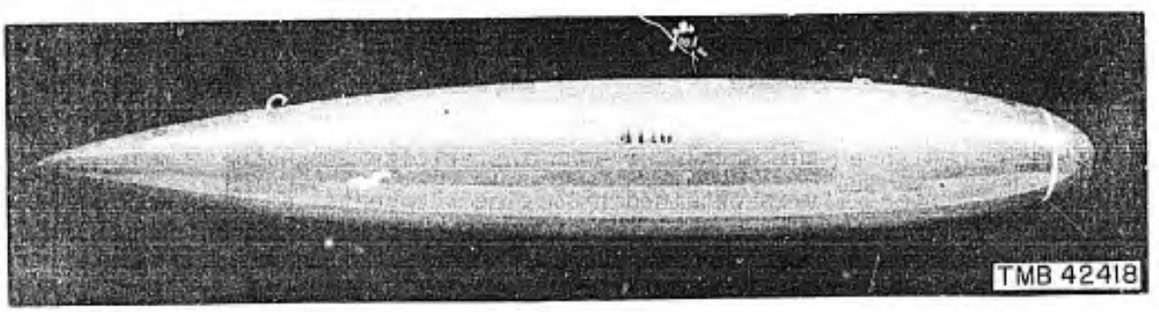

Figure 1 - Representative Model of the Series

the models are listed in Table 1. Offsets and information relative to the mathematical derivation of these forms are given in References 2 and 4. Each form was derived from one of two "parent" forms by variation of a single parameter. Model 4176 was derived from Model 4155, the rest from Model 4157.

TEST APPARATUS

All measurements were made by means of a hydraulic three-component dynamometer, shown schematically in Figure 2. This instrument is described in detail in Reference 5. It was mounted on vertical rails approximately at the

center of Number 3 high-speed towing carriage. These facilities permitted a maximum submergence of approximately 40 inches from the water surface to the top of the model. Lesser depths were obtained by means of spacer struts between the guide rails.

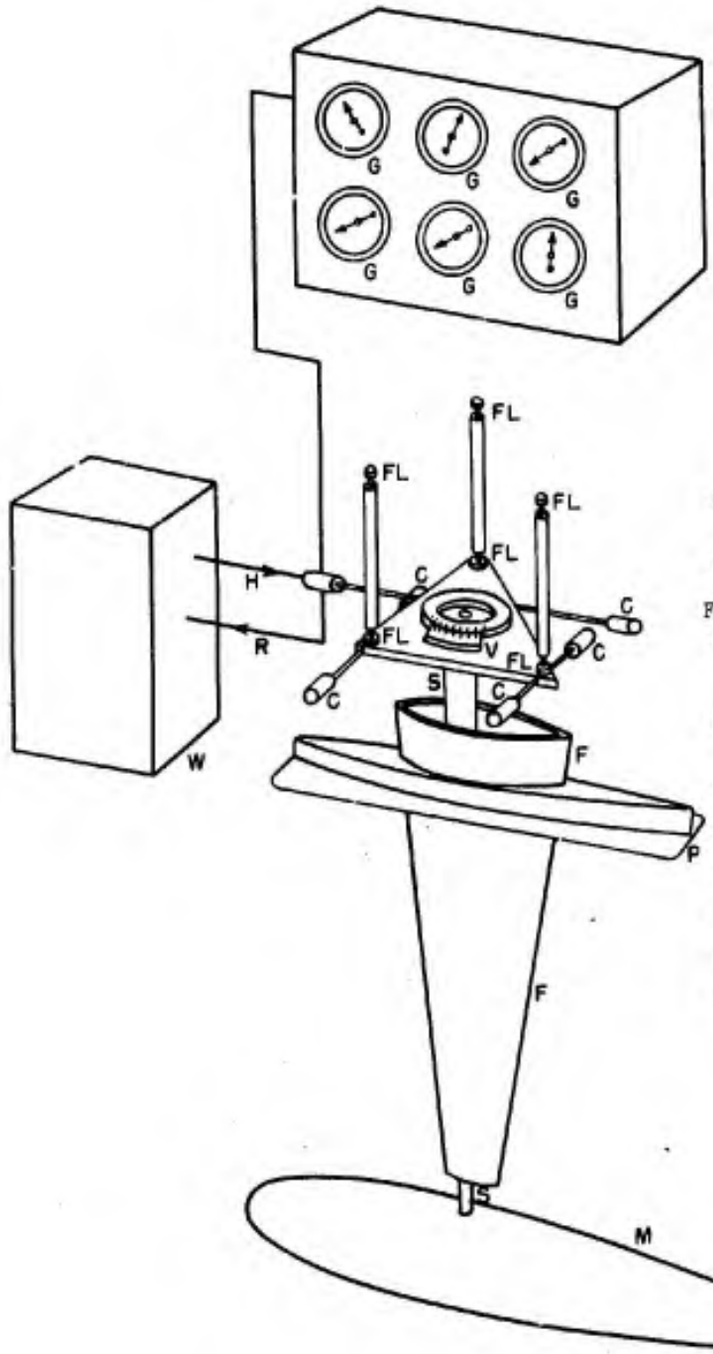

C Pressure capsule, sensitive to axial compressive loads

F Strut fairing, fixed

FL Flexure

G Bourdon gage, one for each pressure capsule

H High-pressure line, one to each capsule

M Model

P Surface plate

R Return line, one from each capsule

S Strut proper

V Angle of attack vernier

W Common source of high-pressure oil: Pump, filters, reservoir and pressure regulator

Figure 2 - Schematic Diagram of 3-Component Dynamometer

TABLE 1

Geometrical Characteristics of Models

Model	l/d	ξ_m	C_p	r_0	r_1	$\bar{x}$	$\forall$ cu. ft.	S sq. ft.
4154	4.0	0.40	0.65	0.50	0.10	0.464	23.26	50.18
4155	5.0						14.89	39.67
4156	6.0						10.34	32.94
4157	7.0						7.60	28.15
4158	8.0						5.82	24.58
4159	10.0						3.72	19.64
4160	7.0	0.36				0.459	7.60	28.20
4161		0.44				0.471		28.14
4162		0.48				0.478		28.14
4163		0.52				0.487		28.16
4164		0.40	0.55			0.430	6.43	25.28
4165			0.60			0.448	7.01	26 81
4166			0.70			0.478	8.18	29.42
4167			0.65			0.490	7.60	27.95
4168				0.30		0.475		28.11
4169				0.70		0.454		28.17
4170				1.00		0.440		28.15
4171				0.50		0.462		28.06
4172					0.05	0.463		28.11
4173					0.15	0.466		28.21
4174					0.20	0.467		28.25
4176	5.0		0.55		0.10	0.430	12.60	35.69
4177	7.0	0.34	0.65			0.458	7.60	28.25

See Notation for explanation of symbols.

As shown in Figure 2, the present dynamometer permits force and moment measurement only in a plane parallel to the surface; hence for longitudinal stability measurements it is necessary to mount a model on its side. The measurements thus taken can more properly be considered as pertaining to a body in yaw; however if surface effects are negligible such measurements may be considered identical to measurements in pitch for an axially symmetric body.

PROCEDURE OF TESTS

All comparative tests, except those for Model 4154, were run at maximum submergence at a carriage speed of 8 knots for angle of attack settings of 0°, ±0.5°, ±1.0°, ±1.5°, and ±2.0°. For Model 4154 the speed was limited to 7 knots owing to the large moments encountered. These speeds gave Reynolds numbers of 12.0×10^6 and 10.5×10^6 respectively, based on the overall length. Supplementary tests were performed on Model 4159 at varied depth and Models 4176 and 4177 at varied speed with and without sand.

RESULTS

Owing to a number of causes, the results obtained are of lower precision than would be desirable for a quantitative appraisal of the models of this series. Among the possible sources of error, the following are the most salient:

1. Strut interference, a condition probably of great importance, which cannot be assessed until the completion of investigations now being made.

2. Small angular range of tests, necessitated by the load limits of the instrument, resulting in a limitation of angle variation to a range of ±2 degrees.

3. Frictionally-restrained lost motion in the instrument, subsequently corrected, but discovered only after completion of the tests herein described.

4. Carriage vibration, resulting in a rapid oscillation of gage pointers about the true reading, a condition for which remedial measures are now being taken.

Owing to the limited submergence permitted by the present three-component dynamometer the question arose as to the effect of surface proximity on lift and moment rates in the horizontal plane. In order to obtain an indication as to the severity of this effect, Model 4159 was towed at 8 knots (Froude number = 0.794), submerged 1.24, 2.00, 3.75, and 4.12 diameters to the center line. Results are shown in Figure 3.

In view of their scatter, the number of test points is too small to permit a quantitative determination of the variation of surface effect with depth. The lift curve is especially difficult to evaluate; however, it is observed that values differing substantially from those for full submergence are displayed only by the smallest depth, 1.24 diameters. At this depth a large air cavity extended behind the towing strut for almost the entire length of the model. It was concluded that the maximum available depth was adequate for

[redacted]

UNCLASSIFIED

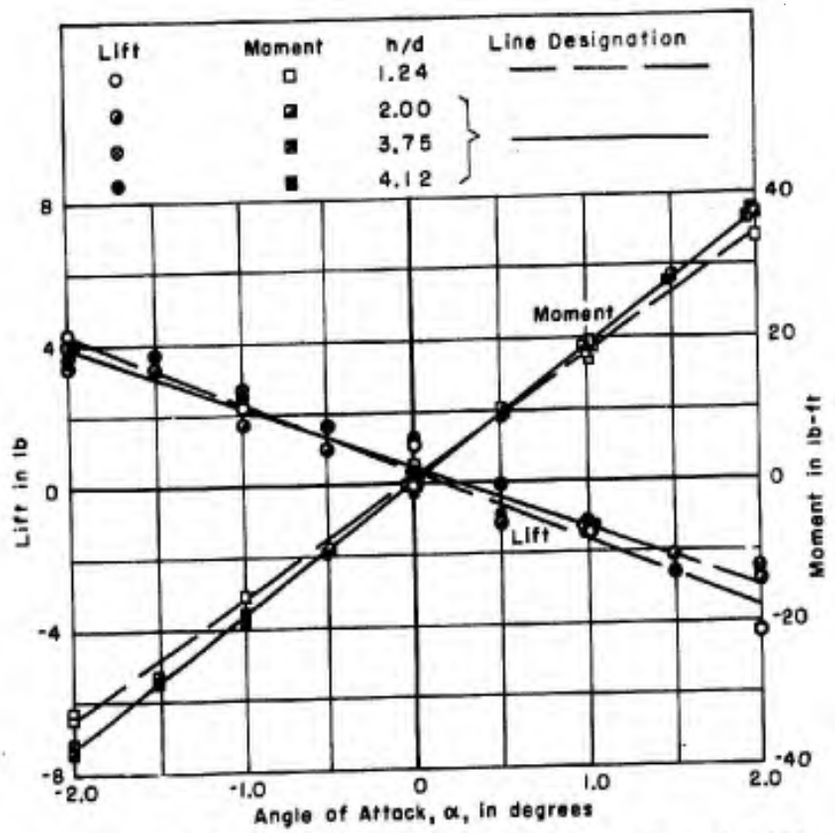

Figure 3 - Model 4159, Variation of Lift and Moment with Depth

Froude number equals 0.794

determination of static derivatives to the accuracy permitted by the dynamometer as then constituted. This conclusion is verified by subsequent more extensive experiments at a slightly lower Froude number, described in Reference 6.

Plots of lift, moment, and drag against angle of attack for a representative model of the series are shown in Figure 4. Values of L'_w and M'_w for each model, evaluated by the method of least-squares from such curves and corrected for torsional deflection of the dynamometer strut, together with values of D' are plotted against form characteristics in Figures 5 through 9.*

*Values of L'_w and M'_w obtained for Model 4157 of sugar pine appear consistently higher than indicated by a line faired through the other model results. This is possibly due to swelling of the model.

UNCLASSIFIED

[redacted]

The normal force derivative Z'_w is readily obtained from these plots by the relationship

$$Z'_w = -(L'_w + D') \qquad [1]$$

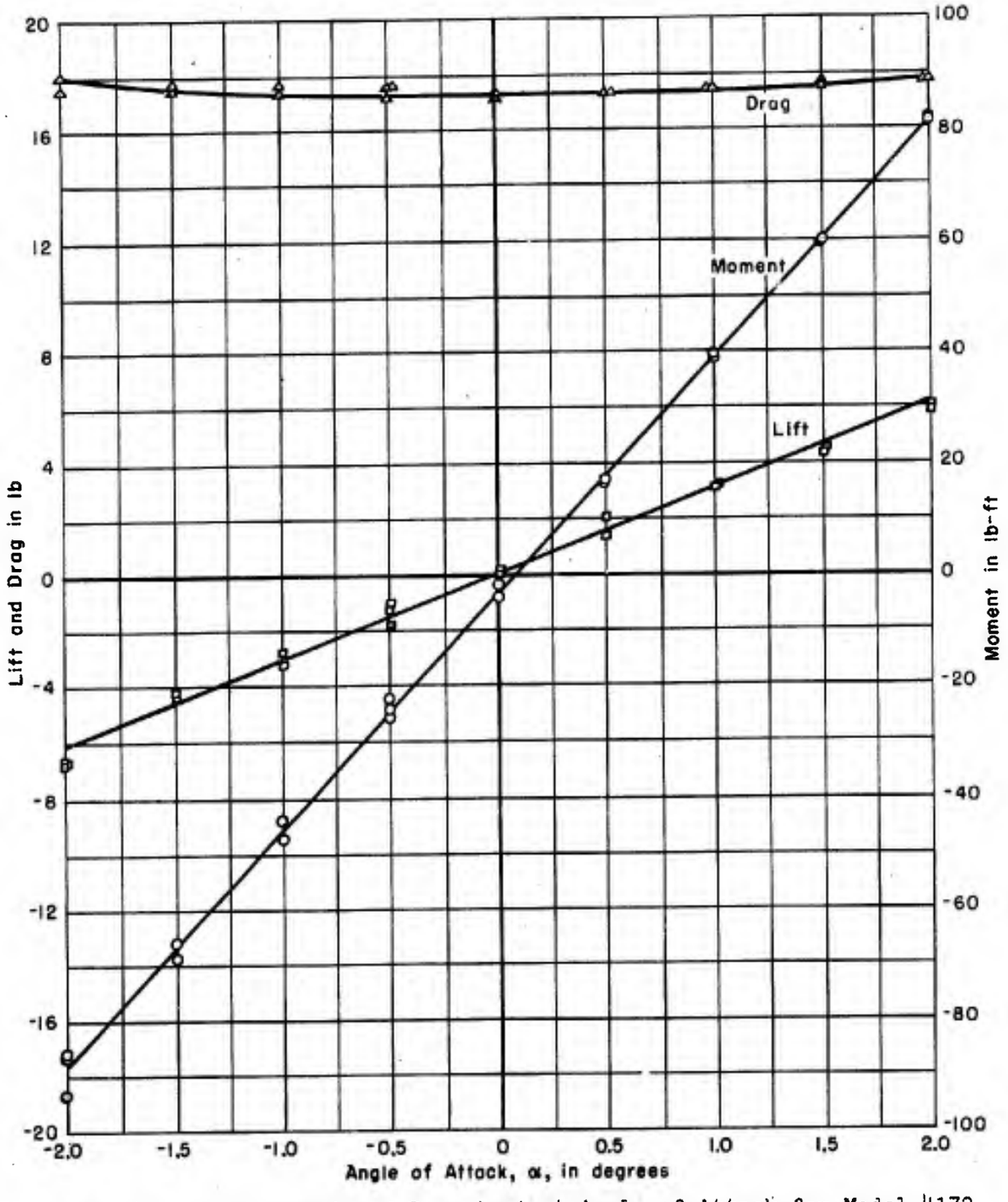

Figure 4 - Lift, Moment and Drag Against Angle of Attack for Model 4172 (Recorded Values, Uncorrected for Torsional Deflection of Strut)

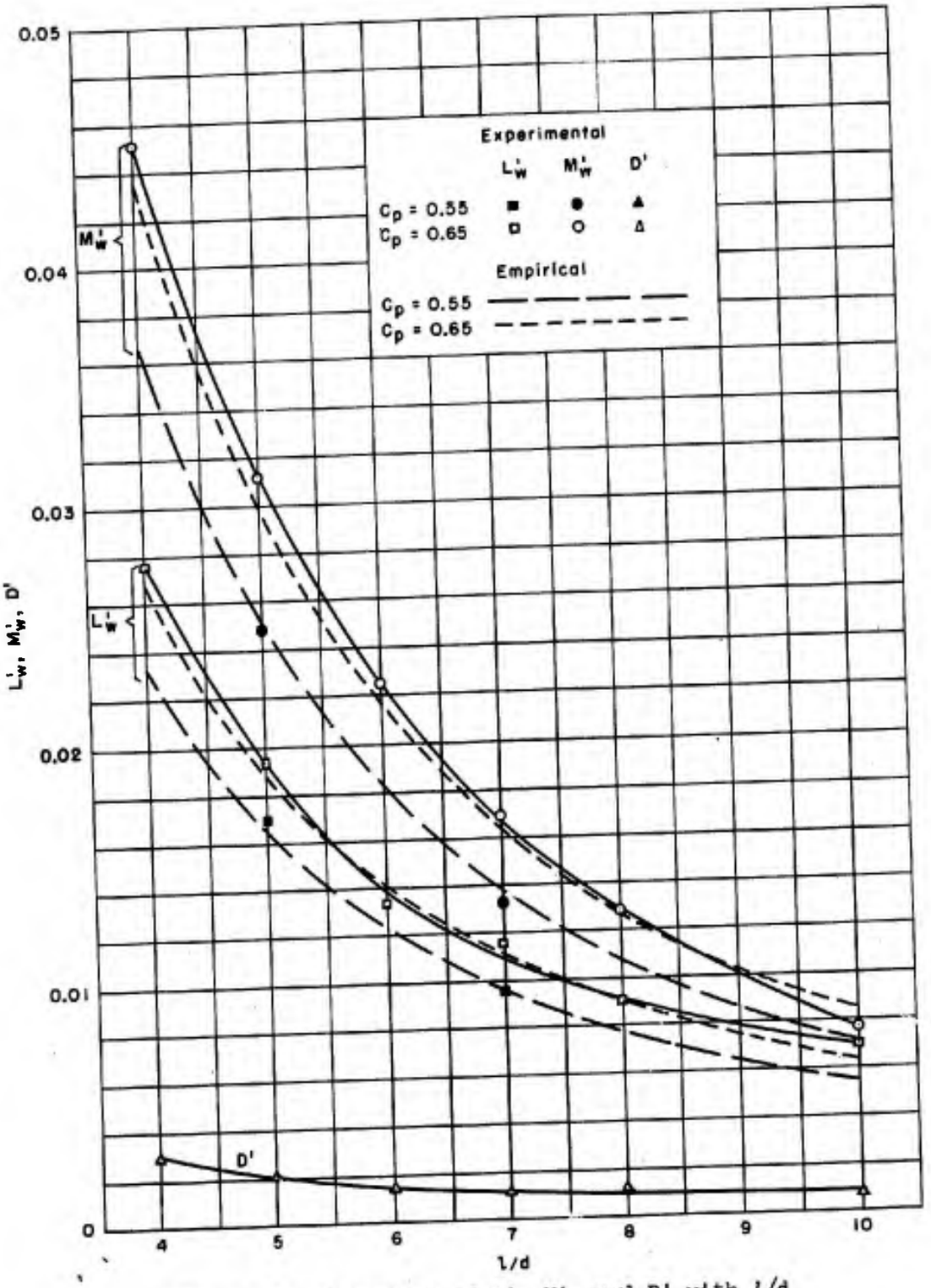

Figure 5 - Variation of L'_w, M'_w, and D' with l/d

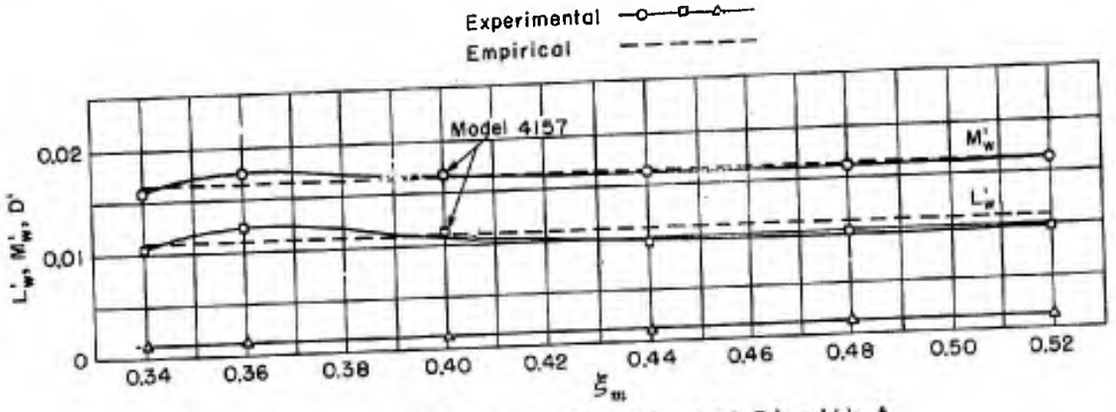

Figure 6 - Variation of L'_w, M'_w, and D' with ξ_m

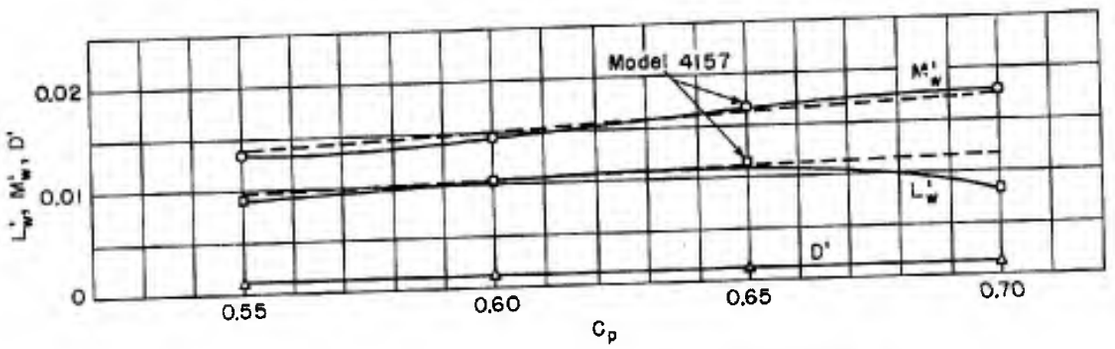

Figure 7 - Variation of L'_w, M'_w, and D' with C_p

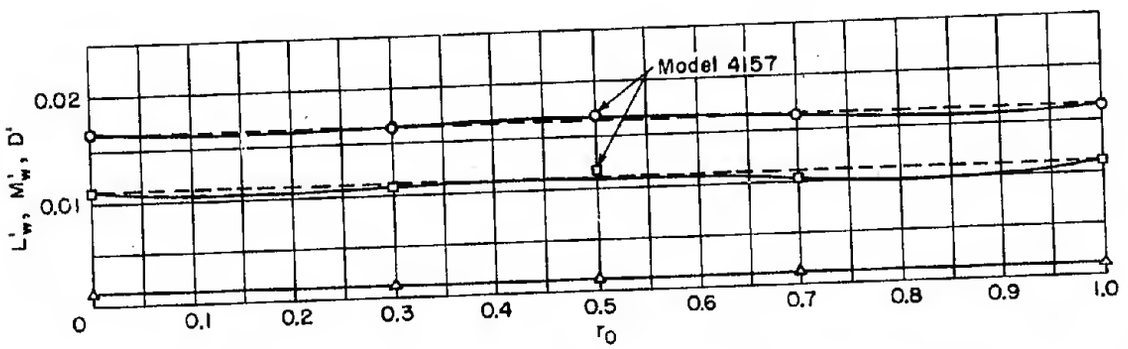

Figure 8 - Variation of L'_w, M'_w, and D' with r_0

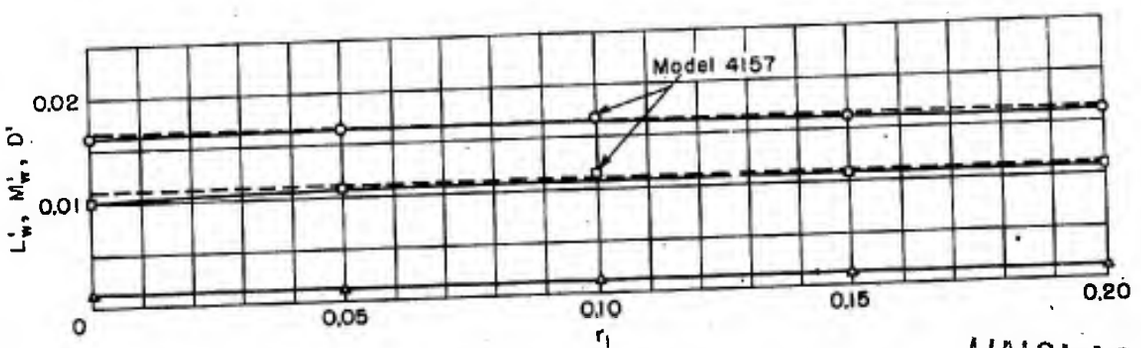

Figure 9 - Variation of L'_w, M'_w, and D' with r_1

More accurate values of D', obtained with sand turbulence stimulation and corrected for strut interference and the resistance of the sand stimulator, can be obtained from the relationship

$$D' = \frac{\pi C_s C_t}{l/d} \qquad [2]$$

C_s, the wetted-surface coefficient, and C_t, the total-drag coefficient, can be obtained from Reference 2. Faired values of L'_w and M'_w are recorded in Table 2.

TABLE 2

Hydrodynamic Characteristics at Zero Angle

Model	Variable	Value of Variable	L'_w	M'_w	M'_{wi}*	$\frac{M'_w}{M'_m}$
4154	l/d	4	0.0276	0.0452	0.0497	0.909
4155		5	.0193	.0312	.0342	.912
4156		6	.0138	.0223	.0248	.899
4157		7	.0108	.0166	.0187	.888
4158		8	.0091	.0128	.0146	.877
4159		10	0.0069	0.0077	0.0096	0.802
4177	ξ_m	0.34	0.0105	0.0157	0.0187	0.840
4160		.36	.0124	.0175	.0187	.936
4161		.44	.0098	.0162	.0187	.866
4162		.48	.0098	.0162	.0187	.866
4163		0.52	0.0101	0.0164	0.0187	0.877
4164	C_p	0.55	0.0091	0.0132	0.0158	0.835
4165		.60	.0103	.0145	.0172	.843
4166		0.70	0.0083	0.0178	0.0201	0.886
4167	r_0	0.0	0.0107	0.0163	0.0187	0.872
4168		.3	.0105	.0162	.0187	.866
4169		.7	.0099	.0161	.0187	.861
4170		1.0	0.0108	0.0160	0.0187	0.856
4171	r_1	0.00	0.0101	0.0162	0.0187	0.866
4172		.05	.0108	.0164	.0187	.877
4173		.15	.0108	.0163	.0187	.872
4174		0.20	0.0108	0.0162	0.0187	.866
4176	C_p@l/d=5	0.55	0.0169	0.0248	0.0290	0.855
Average						0.871

*See Equation [4] which appears in the following section.

To determine if an appreciable change in derivatives with speed occurred in the range of these tests, runs were made at 4, 6, and 8 knots with Models 4176 and 4177 with and without bow sand strip. This strip, 1/2-inch wide, prepared by sprinkling 20-30 mesh sand on a thin adhesive coating, was located 1/20 model length from the nose. Variation of derivatives with speed is shown in Figure 10. Both models show substantial variation in lift derivative over this range and a somewhat smaller variation in moment derivative. For Model 4177 ($l/d = 7$, $\xi_m = 0.34$, $C_p = 0.65$) negligible difference is indicated between runs with and without sand; whereas for Model 4176 ($l/d = 5$, $\xi_m = 0.40$, $C_p = 0.55$) the difference is larger. There are too few points to show with certainty the dependence of the derivatives on speed; however the downward trend and leveling off of the lift-derivative curves indicates that

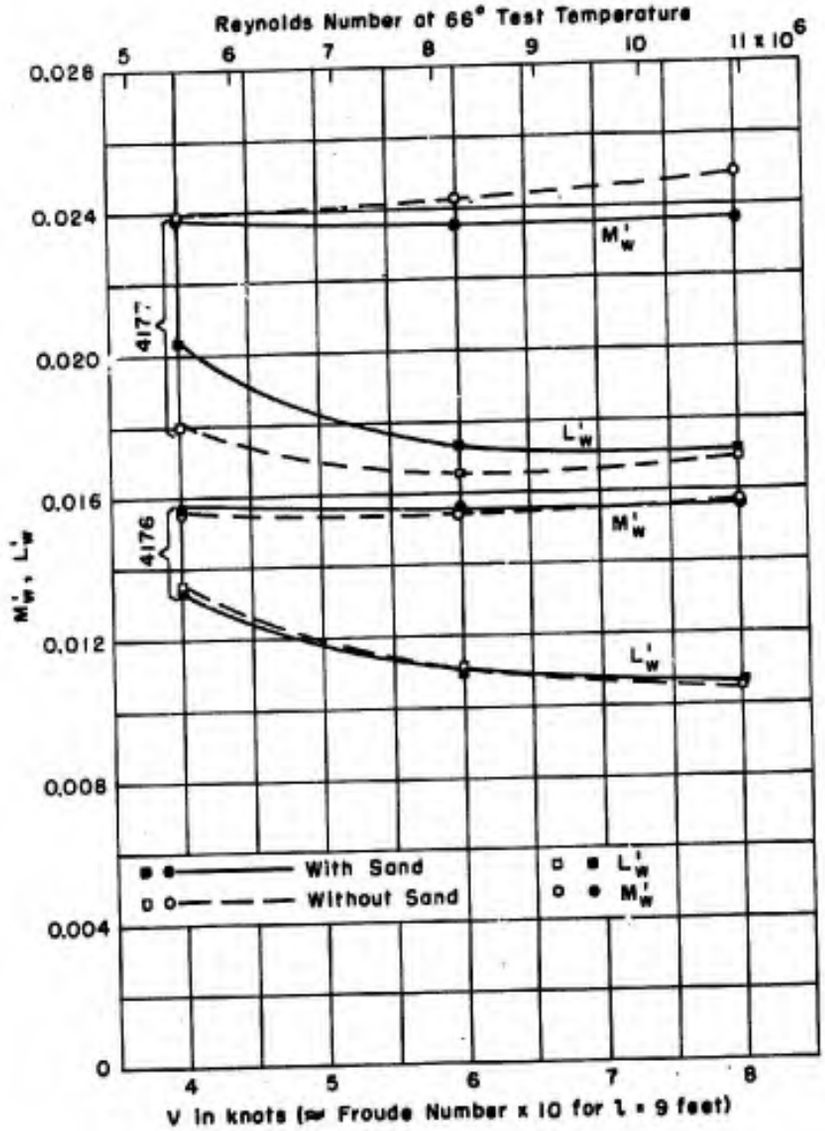

Figure 10 - Variation of Derivatives with Speed

8 knots is probably adequate for obtaining reliable determinations of this quantity for the 9-foot model tested. This downward trend, substantially independent of the presence of sand, indicates that lift for a body of revolution is proportional to some power less than the square of the speed at low Reynolds numbers. Whether this variation with speed would be less pronounced with other means of turbulence stimulation—such as nose wires, turbulence grids or coarser sand—might well be the subject of future investigation.

There is no satisfactory explanation at this time for the divergence of the moment curves for Model 4176 with and without sand or for the relative positions of the lift curves for these conditions.

ANALYSIS OF THE RESULTS

THE MOMENT RATIO; COMPARISON WITH EARLIER TESTS

Munk[7] has shown that in an ideal fluid the moment on a spheroid is given by the expression

$$M_i = \frac{\rho U^2}{2} \forall (k_2 - k_1) \sin 2\alpha \qquad [3]$$

where k_1 and k_2 are Lamb's virtual-mass coefficients (see page 155 of Reference 8), functions of l/d. This theoretical moment appears as a pure couple and the resultant force on the body is zero. For small angles we have, approximately,

$$M_i = \rho U^2 \forall (k_2 - k_1) \alpha$$

Dividing by $1/2\, \rho U^2 \forall^3$ we have the nondimensional expression

$$M_i = \frac{2\forall}{l^3} (k_2 - k_1)\, \alpha = \frac{2\forall}{l^3} (k_2 - k_1) w'$$

or

$$M_{wi} = m'(k_2 - k_1) \qquad [4]$$

where $m' = \frac{2V}{l^3}$ is the dimensionless mass of the displaced fluid.

In a real fluid, however, the moment is less than the value indicated by Equation [3].

If we consider a streamline body of revolution as approximately equivalent to a spheroid of the same length and diameter we can by means of Equation [4], compute for it an approximate value of the ideal-fluid moment. Table 2 shows values of M_{wi} thus computed and the ratio M_w/M_{wi} for the models of this series. Comparison with Table 3, which shows approximate values

TABLE 3

Moment Ratios Given by Previous Model Tests

Model	l/d	C_p	M'_w/M'_{wi}	Source
R101	5.6	0.578	0.809	12
Akron	5.9	0.677	0.838	14
LZ129	6.0	0.665	0.798	12
Fuhrmann	6.1	0.57	0.685	13
LZ120	6.5	0.665	0.719	12
I	7.0	0.68	0.847	13
LZ126	7.24	0.658	0.767	11
LZ127	7.7	0.707	0.824	12
LZ111	8.2	0.685	0.764	12
Average			0.783	

derived by scaling of plots published in References 11 through 14, indicates that the local values are approximately 10 percent higher than the earlier results. Particularly high is the ratio 0.936 recorded for $\xi_m = 0.36$ (TMB Model 4160). This discrepancy is possibly due to strut-interference effects present to a lesser degree in the wire wind-tunnel suspensions of the earlier references. Investigations are in progress to assess and, if possible, to eliminate strut-interference errors.

POSITION OF THE LIFT VECTOR

Harrington[9] demonstrated through wake measurements that the lift of a body of revolution is associated with the vorticity generated by viscous forces on the lee after portion of the body. His measurements and calculations showed that the center of lift is located slightly aft of the center of buoyancy. Its exact position depended on the angle of attack, and was furthest aft at an angle of 12° for the form tested. Englehardt[10] verified the rearward position of the vortex core by observing the rotation of a spinner attached to a search probe. These experimental determinations confirm the fact that lift is associated with vorticity that occurs in a region aft of the center of buoyancy. From the fact that a body in a real fluid exhibits a smaller unstable moment than the ideal fluid value (Equation [3]), it can be inferred that this reduction in moment is due to a countermoment generated by normal components of viscosity-induced hydrodynamic forces. There are four such forces: (a) The resultant force due to the surface friction or boundary

shear, (b) pressure or form drag, (c) lift and (d) induced drag. The line of action of force (a) is uncertain, being influenced by the surface distribution of shear forces; however, it is substantially parallel to the free-stream velocity so that for small angles of attack it may be considered as lying substantially along the body axis. Force (b), also substantially parallel to the body axis, is probably small for well streamlined bodies. Force (c) is perpendicular to the free-stream velocity. For small angles of attack, it can be considered substantially perpendicular to the axis. Force (d), varying approximately as the square of the angle of attack, becoming negligibly small at small angles, acts through the point of application of the lift force and parallel to the free-stream velocity. Thus it appears that it would not be greatly in error to ascribe the total reduction in moment at small angles to the lift alone. Hence we may write

$$aL + M_i - M = 0 \qquad [5]$$

where a is the distance from the center of buoyancy to the lift vector,

L is the lift force,

M_i is the ideal fluid moment given by [3], and

M is the measured moment.

Transposing and placing the quantities in nondimensional form we have

$$a' = \frac{a}{l} = -\frac{M_i' - M'}{L'} \qquad [6]$$

Differentiating numerator and denominator with respect to w and allowing w to approach zero, we have the limiting position:

$$a_0' = -\frac{M_{wi}' - M_w'}{L_w'} \qquad [7]$$

or since

$$M_{wi}' = m'(k_2 - k_1)$$

$$a_0' = -\frac{m'(k_2 - k_1) - M_w'}{L_w'} \qquad [8]$$

With the bow as origin the position is

$$\delta_0' = a_0' - \bar{x} \qquad [9]$$

where $\bar{x}$ is the position of the bow relative to the center of buoyancy. The limiting positions δ_0' of the lift vector for the bodies of the series are given in Table 4. Owing to the relatively large error arising from the sources mentioned earlier in this report, the quantity a_0', which depends upon the difference between the almost equal quantities M_{wi}' and M_w', involves a great deal of uncertainty. Consequently δ_0' is somewhat uncertain. The figures do indicate, however, that δ_0' is approximately 69 percent of the length from the bow for this series.

TABLE 4

Limiting Position of Lift Vector

Model	Variable	Value of Variable	$-a_0'$	$-\delta_0'$
4154	l/d	4	0.163	0.627
4155		5	.155	.619
4156		6	.181	.645
4157		7	.194	.658
4158		8	.198	.622
4159		10	0.275	0.739
4177	ξ_m	0.34	0.286	0.744
4160		.36	.097	.556
4161		.44	.255	.726
4162		.48	.255	.733
4163		0.52	0.228	0.715
4164	C_p	0.55	0.286	0.716
4165		.60	.262	.710
4166		0.70	0.277	0.755
4167	r_0	0.0	0.224	0.714
4168		.3	.238	.713
4169		0.7	.263	.717
4170		1.0	0.250	0.689
4171	r_1	0.00	0.248	0.710
4172		.05	.213	.676
4173		.15	.222	.688
4174		0.20	0.231	0.698
4176	C_p @ l/d=5	0.55	0.249	0.678
Average				0.691

TWO EMPIRICAL RELATIONSHIPS

The local tests show (Table 2) that on the average

$$\frac{M_w'}{M_{wi}'} = 0.871 \qquad [10]$$

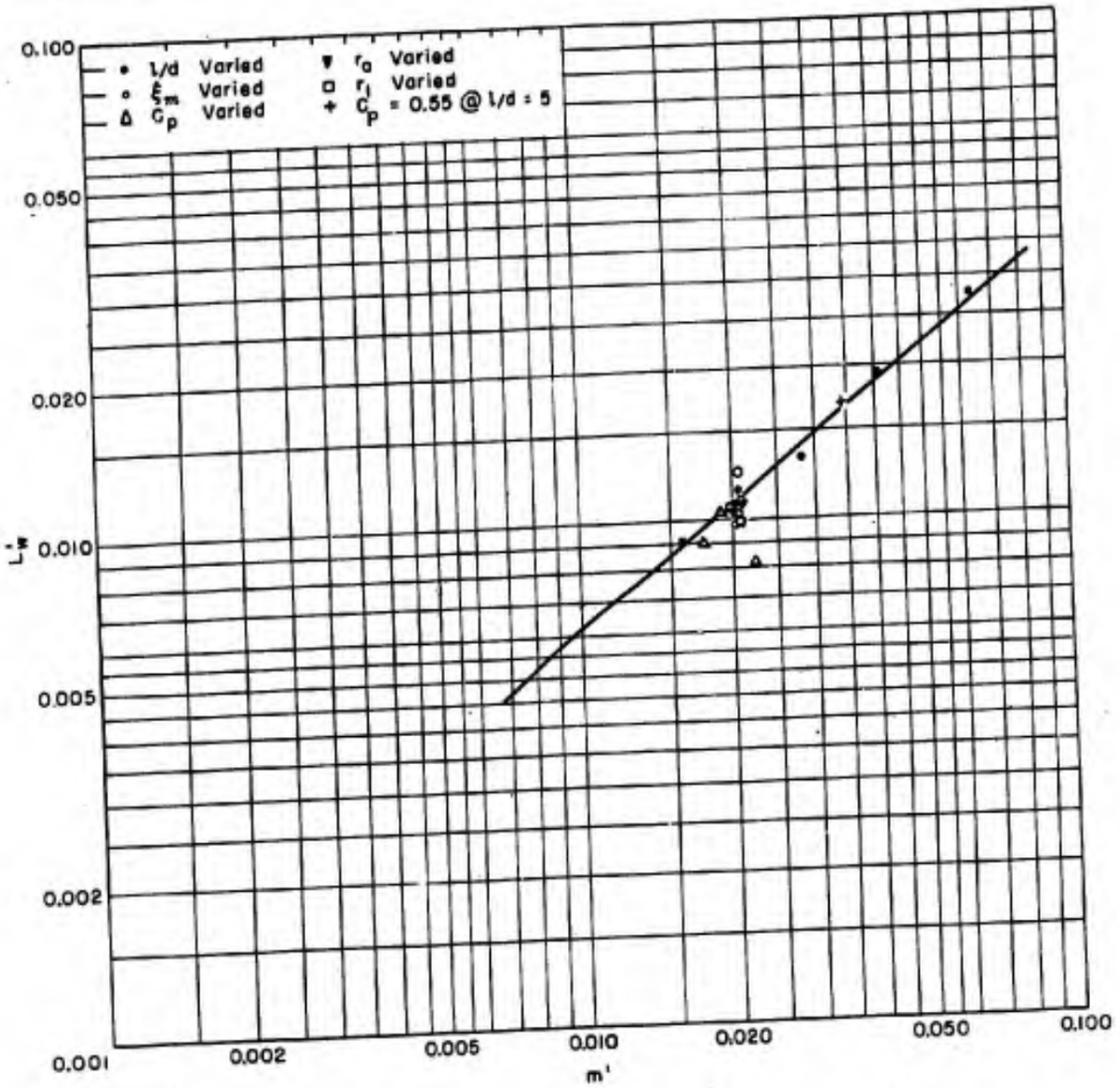

Figure 11 - Logarithmic Plot of L'_w Against m'

so that we have as an empirical approximation

$$M'_{we} = 0.871\ m'(k_2 - k_1) \qquad [11]$$

Values of M'_{we} are plotted as a dotted line in Figures 5 through 9.

Owing to the present lack of a satisfactory analytical approach for determining the lift of an arbitrary body of revolution, an attempt was made to develop an empirical expression that would give results of approximately the same accuracy as Equation [11]. Preliminary studies were made of the variation of L'_w with the following geometrical parameters:

1. (Planform area)/l^2
2. (Frontal area)/l^2
3. (Length x diameter)/l^2
4. (Wetted surface)/l^2
5. $m' = \frac{2\Psi}{l^3}$

These studies showed that the lift derivative could be related most simply to some power of m'. A logarithmic plot of L'_w against m', Figure 11, gives the approximate empirical relationship

$$L'_w = 0.234(m)^{0.79} \qquad [12]$$

Values thus computed are plotted as a dashed line in Figures 5 through 9. Equation [12] is presented as a rapid, approximate means for estimating the lift force on a body of revolution.

CONCLUSIONS

Lift and moment derivatives are greatly affected by variation in l/d and somewhat less by variation in C_p. The effect of ξ_m, r_0 and r_1 is relatively small for the ranges investigated.

Variation in depth of submergence affects the static derivatives only slightly for a submergence of two diameters or more at a Froude number of 0.794.

In order to obtain a boundary flow more closely resembling the full-scale flow it is probably advisable that a bow sand-strip or other means of turbulence stimulation be used. However, a sand strip such as was used in these tests cannot be depended upon to eliminate all variation of derivatives with speed when the Reynolds number is less than 11×10^6.

Based on the results of these tests the following approximate empirical expressions are deduced for the static moment and lift derivatives:

$$M'_{we} = 0.871(k_2 - k_1)m'$$

$$-L'_{we} = 0.234(m')^{0.79}$$

The limiting position of the lift vector as angle of attack approaches zero is approximately 69 percent of the body length from the bow.

The measured moments are generally higher than expected. Strut interference is advanced as a possible explanation. Further investigation is being undertaken to assess and eliminate errors arising from this cause.

REFERENCES

1. BuShips CONFIDENTIAL ltr C-SS/S1-2(420) of 8 July 1949 to TMB.

2. Gertler, M., "Resistance Measurements on a Systematic Series of Streamlined Bodies of Revolution for Application to the Design of High-Speed Submarines," TMB CONFIDENTIAL Report C-297, April 1950.

3. "Nomenclature for Treating the Motion of a Submerged Body Through a Fluid," Technical and Research Bulletin 1-5 of the Society of Naval Architects and Marine Engineers, New York, 1950.

4. Landweber, L., and Gertler, M., "The Mathematical Formulation of Bodies of Revolution," TMB Report 719, September 1950.

5. "Instruments Used in Underwater Stability Investigations at the Taylor Model Basin," TMB Report (in preparation).

6. Brooks, S., Weinblum, G., and Young, D., "Forces and Moment Experienced by a Spheroid Moving Uniformly on a Horizontal Rectilinear Path at and Beneath the Surface." TMB Report (in preparation).

7. Munk, Max M., "Fluid Dynamics for Aircraft Designers," Ronald Press Co., New York, N.Y., 1928.

8. Lamb, Horace, "Hydrodynamics," Sixth Edition, Dover Publications, New York, 1945.

9. Harrington, R.P., "An Attack on the Origin of Lift of an Elongated Body," Publication Number 2, Daniel Guggenheim Airship Institute.

10. Engelhardt, H., "Supplementary Report on Measurements of the Influence of the Fuselage on Tail Surface Effectiveness," Technische Hochschule, Muenchen, April 1943, CADO, Wright Field, Dayton, Ohio, ZWB-THM-1-43A, R3679, F760.

11. Klemperer, W., "Windkanalversuche an einem Zeppelin Luftschiff Model," Abhandlungen aus dem Aerodynamischen Institut an der Technische Hochschule, Aachen, Helf 12, 1932.

12. Schirmer, M., "Aerodynamische Modelversuche an Deutschen und Auslandischen Luftschiff-Baumustern im Windkanl des Luftschiffbau Zeppelin in Friederickschaffen," Doctor's Disertation, Carolo-Wilhamina Technical Institute, Braunschweig, 1942.

13. Hansen, M., "Dreikomponentenmessungen an Drehkörpern mit Verschieden Leitwerken," Forchungsbericht Nr. 1330, Aerodynamische Versuchsanstalt Goettingen, 1941.

14. Freeman, Hugh B., "Force Measurements on a 1/40th Scale Model of the U.S. Akron," NACA Technical Report 432.

NAVY-DPPO PRINC. WASH., D.C.